



Aerodynamics Loads on a Heeled Ship

Romain Luquet, *DGA Hydrodynamics, FRANCE*, romain.luquet@intradef.gouv.fr

Pierre Vonier *DGA Hydrodynamics, FRANCE*, pierre.vonier@intradef.gouv.fr

Andrew Prior, *Royal Canadian Navy, DGMEPM, DNPS 2-3*, andrew.prior@forces.gc.ca

Jean-François Leguen, *DGA Hydrodynamics, FRANCE*, jean-francois.leguen@intradef.gouv.fr

ABSTRACT

Verification of ship stability is based on rules which account for the effects of wind. Restrictive hypothesis are employed to define those rules and especially the influence of ship heeling. This study reviews some stability rules and applies them to the case of the F70 frigate. Then, two alternate approaches are considered: (i) accounting for the actual lateral areas and respective centroids of the heeled ship, and (ii) CFD calculations to determine aero and hydro dynamic coefficients at each heel angle. Finally, comparison is made between the results of these alternate approaches and the stability rules.

Keywords: *wind, CFD, rules, naval ships*

1. INTRODUCTION

Strong winds can increase the risk of capsizing, thus, stability assessment must account for wind effects. This study reviews some of the assumptions commonly embedded in stability rules and investigates two alternate approaches.

1.1 Stability Rules

The first phase of this study was a review of some stability rules (i.e. French Navy, Dutch Navy, IMO, Brown & Dreybach). The formulations defined in these rules were employed to calculate wind heeling moments for the French Navy F70 class frigate.

Whether it is because they are very old (sometimes established more than 50 years ago) or to facilitate the calculations, some of the assumptions common to stability rules are simplistic and do not reproduce faithfully the physics of the studied phenomenon. Examples

of such assumptions include:

Fixed value for aerodynamic drag coefficient regardless of ship geometry or heel angle (e.g. $C_D = 1.12$).

Fixed locations (centroid of projected lateral areas) of application of aero and hydro dynamic forces.

Dead ship condition (zero forward speed with a beam wind) considered the worst case. Blendermann (1996) has shown that beam wind is not the worst case.

Constant wind speed. Gusting is accounted for as either an increase in wind lever arm (IMO) or by defining requirements for righting arm area ratios (naval stability rules).

No variation in amplitude of wind against altitude (IMO) or simple wind profile (naval stability rules). No variation in direction.

Simplified windage area.



1.2 Alternate Approaches

The second phase of this study was to address the first two assumptions of the previous section and investigate two alternate approaches:

AERODYNAMIC APPROACH: Uses the same basic wind moment formulation found in the stability rules. Except, the fixed distance between the upright centroid of windage area and half draft (along with cosine function) are replaced with calculated centroids for above waterline windage area and below waterline hull area (Zaero, Zhydro).

CFD APPROACH: Uses a CFD model to generate aerodynamic and hydrodynamic coefficients (C_Y , C_Z , C_k) for the ship at each heel angle.

1.3 Comparison

The last phase of this study was to compare wind heeling moment results to assess their consistency. The study focused only on the determination of the heeling moment on a ship exposed to a given constant wind speed. The relevance of the choice of speed and associated regulatory criteria is not discussed.

2. STABILITY RULES

1.1 French Naval Rules

The wind heeling moment formula in the French military regulations, IG 6018, (1999) is derived from the work of Sarchin and Goldberg (1962). It requires a reference wind speed (at 10 m height above waterline), assumes a wind speed profile ($\sim h^{1/7}$) and integrates over the projected surface area exposed to wind. Integration is simplified by dividing this surface area into horizontal strips, each being subjected to a constant wind speed depending on the average height of the considered strip.

The inclining lever arm in meters or BLI, due to wind (wind heeling moment divided by $\Delta \cdot g$) is then obtained by summing the influence of each strip as follows:

$$B.L.I. = \sum_i \frac{0.0195 \cdot A_i \cdot h_i \cdot V_i^2}{1000 \cdot \Delta} \cos^2 \varphi \quad (1)$$

Where:

- $V_i =$ Wind speed at strip center [knots]
- $A_i =$ Projected area of each strip [m²]
- $h_i =$ vertical distance between the center of the strip and the drift center (assumed immersed at T/2) [m]
- $\varphi =$ Heel Angle [deg]
- $\Delta =$ Vessel displacement [t]

The coefficient 0.0195 is derived from the combination of physical constants and the units used for wind speed:

$$\frac{1}{2} \frac{\rho C_Y}{g} \left(\frac{1.852}{3.6} \right)^2 = 0.0195 \text{ [kg} \cdot \text{m}^{-2} \cdot \text{kts}^{-2}] \quad (2)$$

Where:

- $C_Y = 1.12$,
- $\rho = 1.29 \text{ kg/m}^3$ and
- $g = 9.81 \text{ m}^2/\text{s}$

The \cos^2 term, which is used in many other regulations, comes from historical studies of sail ships (Middendorf, 1903). Sail ships have a large windage area (upright) that decreases drastically with heel (Middendorf, 1903). The formulation is obviously flawed as at 90° heel a ship will still have a windage area.

1.2 Dutch Naval Rules

The formula used in naval regulations of the Netherlands is similar to the French regulations except that it utilizes a \cos^3 term and does not take into account the wind speed profile. These regulations are derived from Germany naval rules (Arndt 1982). The wind heeling arm formula is as follows:



$$B.L.I. = \frac{P.A.I}{1000.\Delta} \cdot \frac{1 + 3\cos^3(\varphi)}{4}$$

$$P = \frac{C_W \cdot \rho_l \cdot V^2}{2} \quad (3)$$

Where:

P = Wind pressure [Pa]

A = Windage surface area [m²]

I = Distance between the half-draft and the windage area center

$C_W = 1.2$

$\rho_l = 0.125 \text{ kg.s}^2.\text{m}^{-4}$

The advantage of this formulation lies in its ability to model the decay of the heeling moment while maintaining a non-zero value at $\varphi = 90^\circ$. The choice to keep one quarter of the zero heel value seems somewhat arbitrary.

2.3 IMO

In the regulations established by the IMO, and therefore applicable to civilian vessels, the pressure applied on the windage surface is specified instead of the wind speed. In addition, the heeling moment is considered invariant with heel angle. The B.L.I. is calculated as follows:

$$B.L.I. = \frac{P.A.Z}{1000.\Delta.g} \quad (4)$$

Where:

P = Pressure applied to windage surface [Pa]

Z = Distance between the center of the windage area and the center of the underwater lateral area (assumed by default located at T/2) [m]

This formulation is acceptable as it applies mainly to large commercial vessels like container ships or tankers, which by their shape, have a windage surface almost independent of the heel angle.

It is possible to compute an equivalent wind speed by comparing the IMO and naval formula at zero heel. Comparing with the French regulations, the relation obtained is:

$$V = \sqrt{\frac{P}{0.0195.g}} \quad (5)$$

With the usual value of $P = 504 \text{ Pa}$ (IMO without gust) and assuming $C_Y = 1.12$, then $V = 51 \text{ knots}$ or 63 knots (IMO with gust) instead of 100 knots generally used in naval stability rules for combatants.

2.4 Brown & Deybach

Brown & Deybach (1998) proposed a formula that considered the principal dimensions of the ship. Their wind heeling arm formula was as follows:

$$B.L.I. = \frac{\frac{1}{2}C_D\rho V^2 \cdot \left[C_W \frac{L_{PP} \cdot B}{2} + \left(A - C_W \frac{L_{PP} \cdot B}{2} \right) \cos(\varphi) \right]}{1000.g.\Delta} \cdot \left[\frac{B}{2} + \left(L - \frac{B}{2} \right) \cos(\varphi) \right] \quad (6)$$

Where:

C_D = Drag coefficient = 1.12

B = Ship beam

L_{PP} = Ship length

C_W = Water plane area coefficient

3. CASE STUDY

The ship chosen for this study is the French Navy F70 type anti-aircraft frigate shown in Figure 1. The CAD model of the ship used for this study has a simplified superstructure (masts and antennae are not considered) as shown in Figure 2. Blendermann (1999) provides guidance on the influence of the details of the superstructure on the



aerodynamic coefficients and its recommendations have been followed. The hydrostatic characteristics of the hull are presented in Table 1.



Figure 1: French frigate “Jean Bart”

Figure 2: CAD model of “Jean Bart”

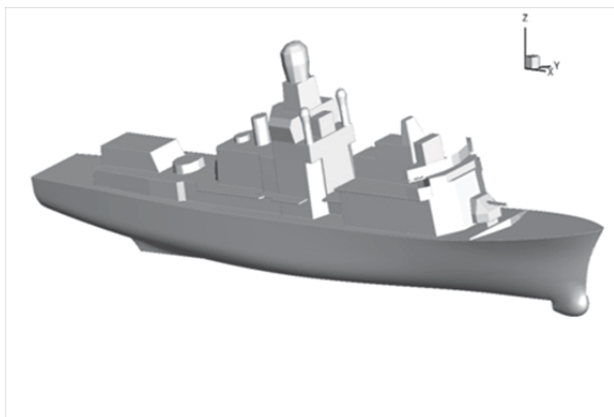


Table 1. Main characteristics

L_{pp}	m	129.00
BWL	m	14.00
T	m	4.82
Δ	t	4873
LCG	m	58.92
YG	m	0.00
VCG	m	5.96

Windage Area	m ²	1346
Z_{aero}	m	6.24
Drift Area	m ²	592
Z_{hydro} / calm water plane	m	-2.37

4. AERODYNAMIC APPROACH (I)

The formulae for wind heeling in the stability rules (other than IMO) use the aerodynamic drag at zero heel angle (or at best taking into account variation using \cos^2 or \cos^3 functions). In addition, they assume that the drift center is located at half draft.

One way to improve upon these formulae is to remove the assumption of an a priori law of decrease (\cos^2 or \cos^3) by calculating the actual projected windage area and centroid height (Z_{aero}) and immersed lateral area and centroid depth (Z_{hydro}) at each heel angle. The wind heel lever formula is thus:

$$B.L.I. = \frac{1}{2} \frac{C_Y \cdot A \cdot (Z_{aero} - Z_{hydro}) \cdot V^2}{1000 \cdot \Delta \cdot g} \quad (6)$$

Where:

V = Wind speed [m/s] (at height Z_{aero})

$C_Y = 1.12$

$\rho = 1.29 \text{ kg/m}^3$

A , Z_{aero} , Z_{hydro} are calculated at each heel angle. This done by using FASTABI (DGA hydrodynamics code) to establish the hull equilibrium position (waterline position relative to hull) at each heel angle and then using the CAD model to calculate projected areas and centroids. Figure 3 illustrates this procedure.

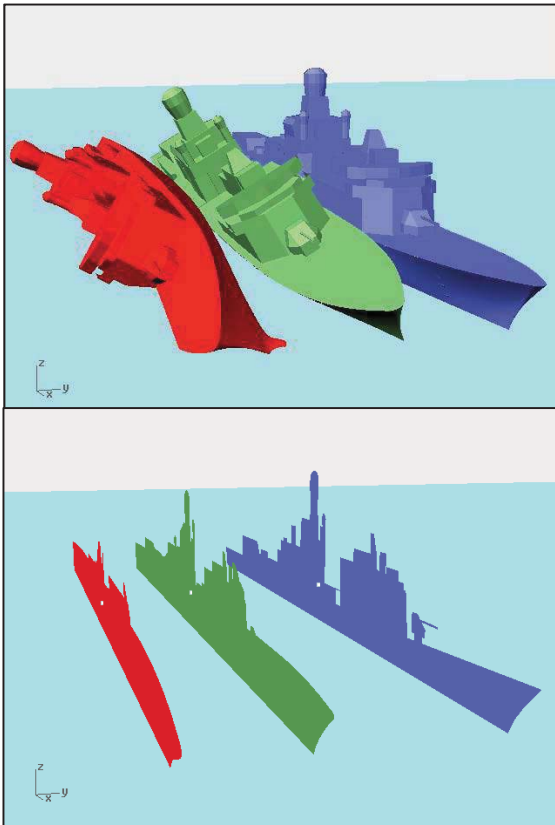


Figure 3: equilibrium and projected wind areas

Figure 4 plots wind lever results for this alternate approach along with the results obtained using the stability rule formula noted in Section 2. To ensure likewise comparison, a wind speed of 100 knots at 10m has been used in all cases, Equation (5) was used to calculate the corresponding pressure for the IMO formula.

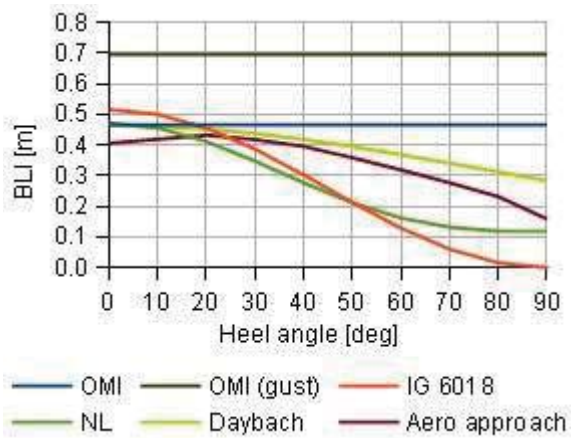


Figure 4: comparisons of BLI

At zero heel, BLI values are all quite similar. However, the shape of the lever arm curves (variance with heel) is very different. This alternative approach shows a maximum around 20° heel angle.

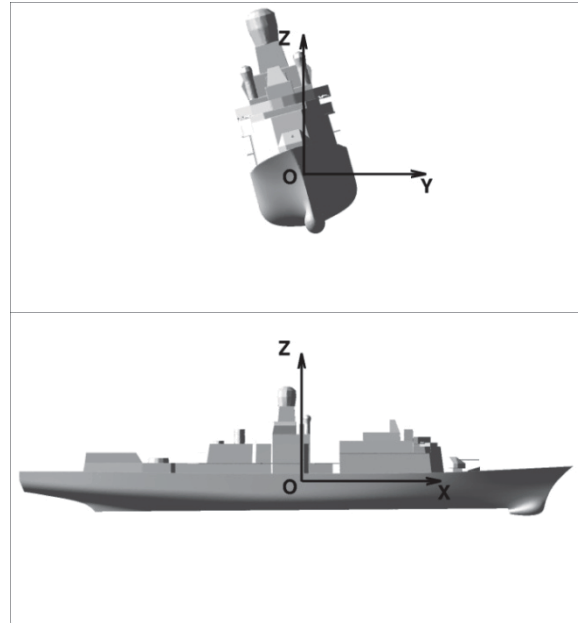


Figure 5: coordinate systems

5. CFD APPROACH (II)

CFD simulations were performed in a dead-ship condition to determine the aero and hydro dynamic forces acting on the ship.

5.1 Coordinate System & Coefficients

CFD work was conducted using the fixed coordinate system shown in Figure 5. The axes are independent of the heel angle, only the position of the origin is linked to the ship. The origin is located as follows:

- O_x : At ship LCG (+ fwd, - aft)
- O_y : At ship Centreline (+port, -starboard)
- O_z : At the waterline (+above, -below)

The coefficients C_Y , C_Z and C_K are defined as:



$$\begin{aligned}
 C_Y &= \frac{F_Y}{\frac{1}{2} \rho U_{ref}^2 S_{ref}} \\
 C_Z &= \frac{F_Z}{\frac{1}{2} \rho U_{ref}^2 S_{ref}} \\
 C_K &= \frac{M_X}{\frac{1}{2} \rho U_{ref}^2 S_{ref}^2 / L_{ref}} \quad (7)
 \end{aligned}$$

Where:

F_Y, F_Z = Force experienced by the ship in the y-axis and z-axis respectively.

M_X = Is the heeling moment acting on the ship (rotation about the x-axis).

L_{ref} = Ship length between perpendiculars.

Depending on whether aero or hydrodynamic forces are being considered:

S_{ref} = Either projected windage area or submersed hull area at zero heel angle.

U_{ref} = Wind speed or drift velocity.

ρ = Air or water density.

5.2 Computational domain and mesh

The computational domain is a parallelepiped as illustrated in Figure 6. A velocity-inlet condition (red) is applied on the upstream boundary and a pressure-outlet condition (blue) is applied at the downstream boundary. A no-slip condition (green) is imposed on the ship and a symmetry condition (gray) on the other boundaries. The computational domain covers $3 L_{pp}$ on each side and $1.5 L_{pp}$ above and below the ship.

The mesh consists of 17 million calculation points constituting 5 million polyhedral cells. The mesh near the walls is made of prisms to ensure proper computation of the boundary layer. The non-dimensional distance from the wall y^+ is fixed at 50 on the hull. The mesh is also made of prisms at the free surface to allow an accurate resolution in this crucial area. The rest of the mesh is covered by polyhedra.

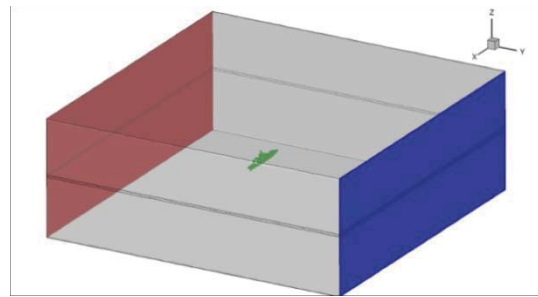


Figure 6: computational domain

5.3 Numerical Method

The calculations were performed using the commercial software FLUENT from ANSYS. It solves RANS equations (Reynolds Averaged Navier-Stokes equations). For these calculations, the Volume Of Fluid (VOF) model was used to simulate the coexistence of the two fluids (air and sea water). A $k\omega$ -SST model was used to model the turbulence of the two fluids.

The simulations are unsteady using an adaptive time step beginning at 0.1s to reach 1s at the end of the calculation. High order discretization schemes have been applied to the momentum equations (MUSCL) and volume fraction (HRIC) to allow an accurate resolution of the air-water interface. The hull was considered to be hydraulically smooth (roughness was not taken into account).

5.4 Calculation Conditions

The simulations were performed on flat sea for a ship at zero forward speed in a fixed position according to the hydrostatic equilibrium at the selected heel angle (the equilibrium is only satisfied on the heave).

The characteristics of the two fluids simulated are shown in Table 2. The fluid properties were constant over the computation domain and the effects of temperature, pressure and air hygrometry were neglected.

Table 2. Main characteristics of fluid



Salt water (15°C)			
Dynamic viscosity	μ	(Pa.s)	$1.2200 \cdot 10^{-03}$
Density	ρ	(kg/m ³)	1026
Speed	V_{hydro}	(m/s)	Such that $F_y=0$
Air (15°C, 1% RH, 1013 mbar)			
Dynamic viscosity	μ	(Pa.s)	$1.7894 \cdot 10^{-05}$
Density	ρ	(kg/m ³)	1.225
Wind speed at 10m	V_{aero}	(knots)	100

A uniform lateral current was applied to the flow (water) to model the consecutive drift of the ship due to the efforts of the crosswind. The current speed was determined by balancing the drift forces sustained by the ship (aerodynamic and hydrodynamic loadings). The heeling moments balance is not verified.

Inlet condition imposed on the airflow was determined to correspond to a fully developed turbulent boundary layer profile. For a 100knot wind (at 10m reference height), the turbulent intensity at 10m is of the order of 10%. Theoretical profile, up- and down- stream computed profiles are shown in Figure 7.

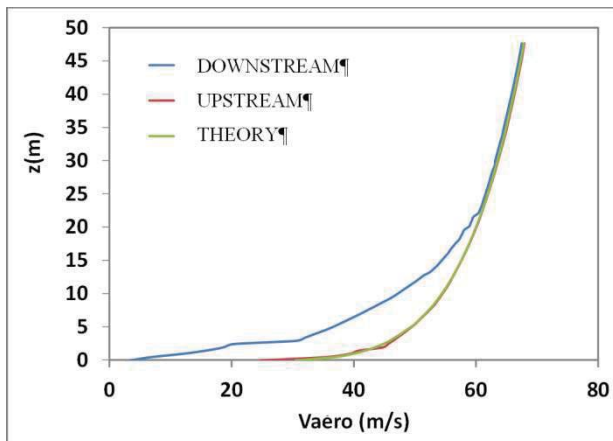


Figure 7: wind profile

5.5 Sensitivity and Convergence

A limited sensitivity analysis was performed. Firstly a higher density of mesh (10 million polyhedra) was tested to quantify the

influence of the discretization of the computational domain. A maximum variation of about 3% was observed on the force coefficients. Then the upstream turbulence flow rate was multiplied and divided by two without observing any significant influence on the results. An evaluation of the influence of Reynolds number was also performed. Computations were performed for different wind speeds at zero heel angle, the results are shown in Table 3. There were no significant changes in the aerodynamic force coefficients; as expected since the Reynolds number remains greater than 10^7 .

Table 3. Main characteristics of fluid

V knots	R_e	C_Y	C_Z	C_K
25	$1.23 \cdot 10^{+07}$	0.86	0.65	0.44
50	$2.47 \cdot 10^{+07}$	0.84	0.64	0.45
100	$4.93 \cdot 10^{+07}$	0.83	0.62	0.47

The simulation duration was a period of 500 s which allowed good convergence of the force and moment coefficients as shown in Figure 8. Coefficient values reported in this study are the average over the last hundred seconds of simulation.

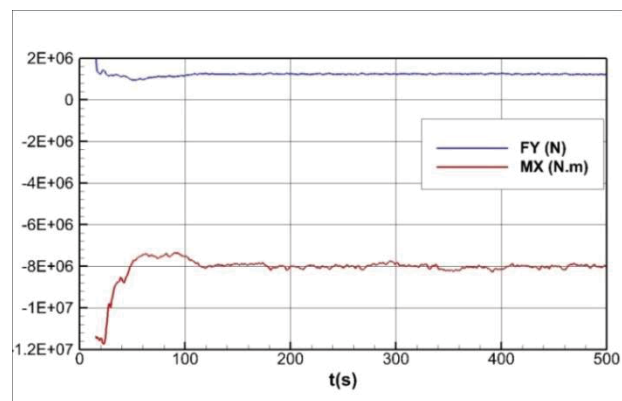


Figure 8: force and moment time trace

The CFD calculation methodology used for this study has not been validated using a



verification procedure. However, some confidence may be taken from comparison of the results obtained to data from wind tunnel tests. Blendermann (1996, 1999) conducted zero heel angle tests for two ships with silhouettes similar to that of the F70 frigate (see Figure 9). Table 4 presents the C_Y and C_K coefficients from CFD and the Blendermann tests.

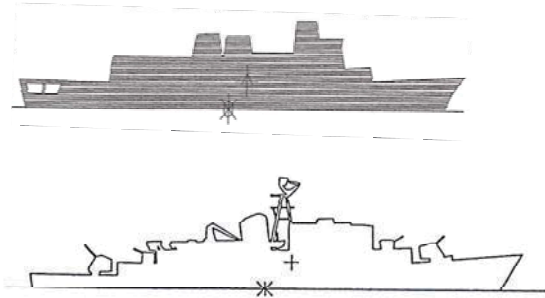


Figure 9: From Blendermann (1996 and 1999)

Table 4. Comparison with Blendermann

	F70 Present CFD	Blendermann Tests	
		1996	1999
C_Y	0.83	0.81	0.85
C_K	0.47	0.48	0.49

Finally, a procedure for CFD simulation has been developed to evaluate the hydrodynamic and aerodynamic loads for vessel in the deadship condition (zero forward speed and drifting in a beam wind); see Figure 10 & 11.”

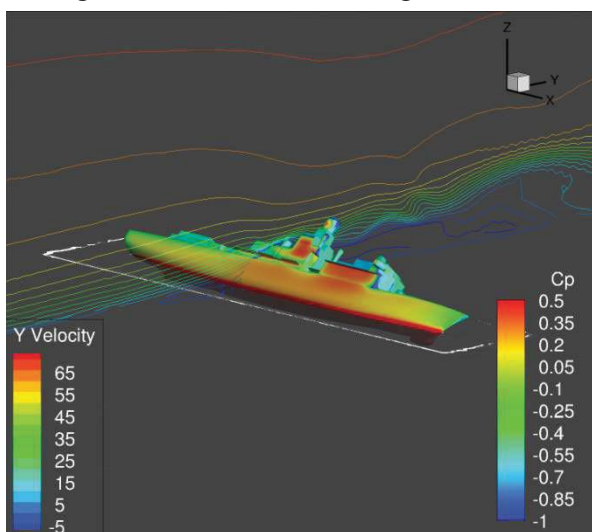


Figure 10: Iso-contours of C_p and iso-lines of transverse speed (m/s) around frigate F70 at $+45^\circ$ heel angle

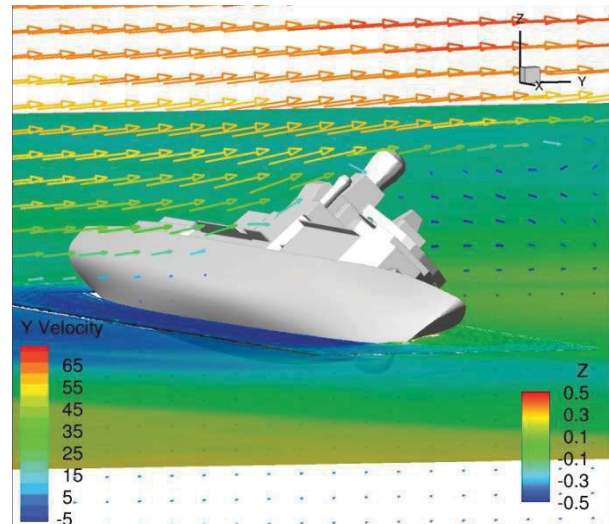


Figure 11: Iso-contours of $Z(m)$ and transverse speed (m/s) around frigate F70 at $+45^\circ$ heel angle

5.6 Results

A series of simulations were performed for a wind speed of 100 knots and heel angles ranging from -60° to $+60^\circ$; the positive heel angles correspond to the realistic situation where the ship leans towards leeward. The resulting force and moment coefficients are shown in Figure 12. There is a decrease in C_{Zaero} , C_{Yaero} and C_{Yhydro} with increasing heel angle. Note also that C_{Zaero} and C_{Yhydro} are of the same order of magnitude. C_{Zaero} will influence roll moment because the pressure field on the deck and superstructures of the ship is not symmetrical; this influence is not accounted for in the stability rules reviewed.

Figure 13 shows the vertical location of the point of application of the aerodynamic and hydrodynamic forces. As expected, the point of application of aerodynamic force is located near the centroid of the projected windage area and its height decreases with increasing heel angle. The position of the point of application



of hydrodynamic forces is above the free surface at zero heel but moves below with increasing heel angle to approach the mid-draft position. The heeling moment lever arm, $z(\text{aero}) - z(\text{hydro})$, does not change greatly with heel angle.

Table 5 presents drift velocity (V_{hydro}) and the lateral force coefficients $C_{Y\text{hydro}}$ and $C_{Y\text{aero}}$ for each heel angle. There are little variations in $C_{Y\text{hydro}}$ and $C_{Y\text{aero}}$ and thus V_{hydro} over the range of heel angles.

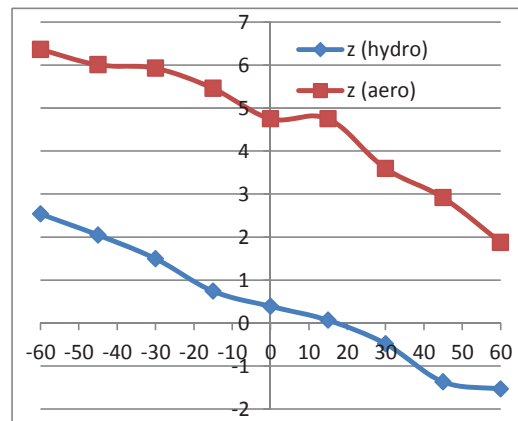


Figure 13: vertical location of hydro and aero forces

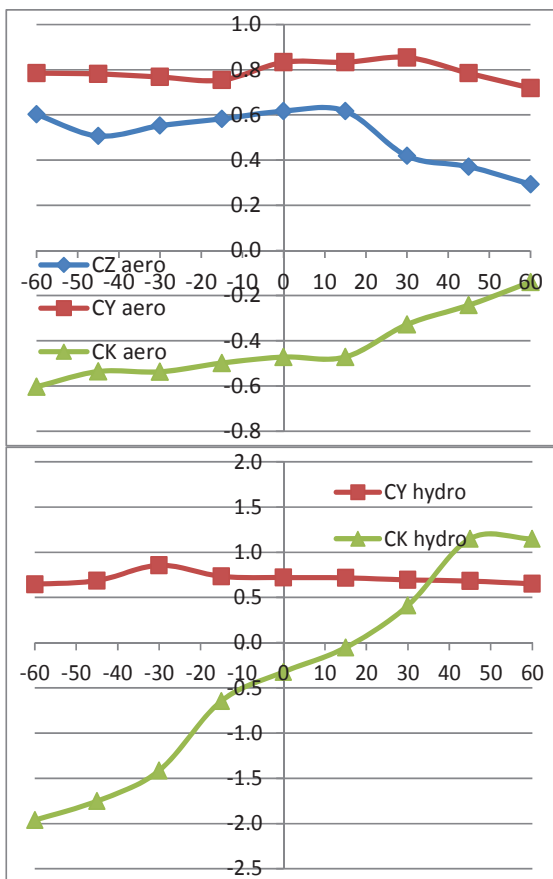


Figure 12: force and moment coefficients for different heel angles

Table 5. Drifting speeds for 100 knots of wind

Heel (°)	CY hydro (-)	CY aero (-)	V hydro (knots)
-60	0.65	0.78	5.7
-45	0.69	0.78	5.6
-30	0.85	0.77	5.0
-15	0.73	0.75	5.3
0	0.72	0.83	5.6
15	0.72	0.83	5.6
30	0.69	0.85	5.8
45	0.68	0.78	5.6
60	0.65	0.72	5.5

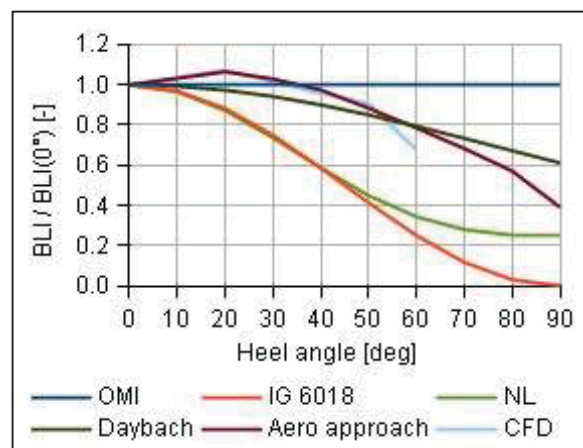


Figure 14: BLI comparisons



6. COMPARISON

Figure 14 presents comparison of the aerodynamic approach and the CFD approach to the stability rules reviewed. Since wind speed and formulation in the rules vary, the curves have been made non-dimensional using values for zero heel. The shape of the aerodynamic and CFD approach curves match well and show a maximums at 20° and 15° respectively. The decrease in BLI is much less pronounced than that obtained by the \cos^2 and \cos^3 function formulae found in the stability rules.

7. CONCLUSIONS

A review was made of different stability rule formulae to account for the effects of wind heeling. These formulae have been applied to the case of F70 frigate. The results obtained were compared to those derived from two alternate approaches. The first approach adopted the same basic formula of the stability rules but replaced the fixed upright windage area, centroids and \cos^2 terms with actual areas and centroids determined for each heel angle. The second approach employed CFD analysis to determine force and moment coefficients at each heel angle. A procedure for CFD simulation has been developed to evaluate the hydrodynamic and aerodynamic loads for vessel in the deadship condition (zero forward speed and drifting in a beam wind).

For the F70 frigate, the two alternate approaches produced similar BLI results. The BLI versus heel angle curves for both have a significantly different shape than that derived from stability rule formula based on a \cos^2 law. Of particular note is that both approaches show a peak in BLI (maximum destabilizing moment) in the 15° to 20° range of heel.

The alternate approaches presented here are interesting and deserves further study. In particular, further work can be done to improve the accuracy of the CFD simulations and

validate the results obtained. This would provide the tool necessary for more comprehensive analysis leading to improved stability rule formulae.

ACKNOWLEDGMENTS

This study was based on CRNAV (Cooperative Research Navies) discussions. Thanks also to H el ene Eudier who started the work in Val de Reuil during a training course. For the French part, the study is funded by the French Ministry of Defence to support DGA Hydrodynamics in its research activities.

REFERENCES

- Arndt B., H. Brandl and K. Vogt, 1982, 20 years of experience – Stability regulations of the West-German Navy, STAB'82, Tokyo pp. 111-121.
- Blendermann W., 1999, Influence of model details on the wind loads demonstrated on a frigate, in Schiff & Hafen.
- Blendermann W., 1996, Wind loadings of ships, - collected data from wind tunnel tests in uniform flow, Institute of Naval Architecture.
- Brown A.J. and Deybach F., 1998, Towards a rational intact stability criteria for naval ships, Naval Engineers Journal.
- DGA/DSA/SPN IG 6018 indice A, 1999, Stabilit e des b atiments de la Marine.
- Middendorf, 1903, Bemastung und takelung des schiffe.
- MSC.267(85).
- Sarchin & Goldberg, 1962, Stability and buoyancy criteria for US naval surface ship, SNAME transactions, vol 70 pp418-434.